CHEMISTRY OF MATERIALS
Cite This: Chem. Mater. 2018, 30, 2208−2212
Communication
pubs.acs.org/cm

Organosilica with Grafted Polyacrylonitrile Brushes for High Surface Area Nitrogen-Enriched Nanoporous Carbons

Jianan Zhang,[†,‡,§] Yang Song,[‡,∥] Yepin Zhao,[†] Shuo Zhao,[‡] Jiajun Yan,[‡] Jaejun Lee,[†] Zongyu Wang,[‡] Siyuan Liu,[†] Rui Yuan,[‡] Danli Luo,[†] Maciej Kopeć,[‡] Eric Gottlieb,[‡] Tomasz Kowalewski,[‡] Krzysztof Matyjaszewski,[*,‡] and Michael R. Bockstaller[*,†]

[†]Department of Materials Science and Engineering and [‡]Department of Chemistry, Carnegie Mellon University, Pittsburgh, Pennsylvania 15213, United States

[§]School of Chemistry and Chemical Engineering, Anhui University and Anhui Province Key Laboratory of Environment-friendly Polymer Materials, Hefei 230601, China

[∥]Collaborative Innovation Center of Advanced Nuclear Energy Technology, Institute of Nuclear and New Energy Technology, Tsinghua University, Beijing 100084, China

Supporting Information

Heteroatom-doped nanoporous carbons (NPCs) have been extensively investigated in multiple energy and environmental applications, including electrode materials for batteries, supercapacitors, fuel cells, catalyst supports, and CO_2 capture.[1−6] Ideally, NPC materials should exhibit both a high specific surface area (SSA) and high heteroatom content to achieve high efficiency in electrochemical applications. Depending on the type of the template, NPCs can be obtained through either soft- or hard-template strategy.[7] The soft-template approach utilizes the self-assembly of the polymer precursors and retains the structure upon carbonization.[7−15] However, such strategy is usually restricted by low yield, relatively high cost, the difficulty to obtain ordered structures, and availability of proper templates. The ability to better control the microstructure of the resulting porous carbon has motivated interest in the hard template approach. Examples include silica-templated NPCs,[16−20] polyhedral oligomeric silsesquioxane moieties,[21] mesoporous silica,[22,23] and porous metal−organic frameworks (MOFs).[24]

Commercial colloidal silica can act as a hard template for the fabrication of NPCs because of its economic viability and amenability to surface modification. Especially, surface-grafting techniques were successfully employed to modify the surface of silica nanoparticles (NPs) to yield polymer-tethered particles which processed into structurally uniform "one-component" hybrid materials that were subsequently pyrolyzed.[25−32] The resulting NPCs exhibited excellent uniformity of pore microstructures.[33−35] For example, polyacrylonitrile (PAN) was synthesized by grafting from silica (d = 15 nm) using surface-initiated atom transfer radical polymerization (SI-ATRP) to generate NPCs with a SSA of 450 m^2/g. To further enhance the SSA, utilization of smaller particle size has been attempted. However, SI-ATRP methods remain challenging for sub-10 nm silica NPs due to the difficulty of aqueous phase immobilization an ATRP initiator on their surfaces. Reduced initiator binding efficiency for smaller particles and aggregation will occur during the transfer into organic solvents, which is needed for initiator immobilization. Therefore, fabrication of NPCs with higher SSA using smaller silica NPs as a template still remains a challenge.

Herein we report on a novel and versatile approach for the synthesis of nanosized polymer-tethered silica particles for hard-templating of NPCs with SSA exceeding 1000 m^2/g.[34−36] This technique is based on the direct synthesis of Br-containing organosilica NPs with diameter <5 nm using a brominated organosilica precursor and the subsequent PAN grafting to prepare silica-*g*-PAN composites by SI-ATRP without further modification or purification. Well-defined NPCs were obtained after carbonization and HF etching, providing a high SSA (1244 m^2/g) and a high nitrogen content (11.9 wt %). The electrochemical properties of the as-prepared NPCs were investigated to evaluate their potential applications as high-performance supercapacitors. Given the facile synthesis of NPCs from controlled silica sizes and adjustable PAN length, the method employed here is expected to allow the systematic design of various NPCs with controlled microstructures.

Figure 1 illustrates the preparation process of NPC with a high SSA from initiator-functionalized organosilica NPs. In the first step, a tetherable ATRP initiator, 6-(triethoxysilyl)hexyl α-bromoisobutyrate was synthesized (Scheme S1).[37] Then, initiator-functionalized organosilica NPs of various sizes were prepared in different organic solvents (Figure 1a, Scheme S2). The sizes of organosilica NPs prepared using methanol, acetone, and DMF as solvents were 3, 25, and 450 nm, respectively (Figures S1 and S2). Furthermore, a seed growth method was adopted to prepare larger organosilica NPs in methanol with average diameters of 3, 5, and 9 nm (Figure S3). Subsequently, silica-*g*-PAN with different brush lengths were prepared by SI-ATRP (Figure 1b), which was confirmed by TEM and thermogravimetric analysis (TGA) (Figures S4−S6). NPCs were obtained after the carbonization of SiO_2-*g*-PAN composites and the complete etching of silica cores (Figure 1c).

TGA analysis was performed to confirm the composition of organosilica NPs and SiO_2-*g*-PAN hybrids, which is shown in Figure 2. In the case of organosilica NPs, the weight loss (42.1 wt %) was associated with its calculated composition, assuming

Received: February 6, 2018
Revised: March 15, 2018
Published: March 20, 2018

DOI: 10.1021/acs.chemmater.8b00577
Chem. Mater. 2018, 30, 2208−2212

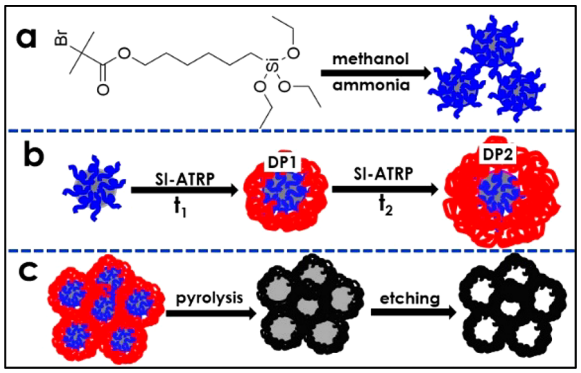

Figure 1. Scheme for the preparation of NPCs using SiO_2-*g*-PAN hybrids as templates by SI-ATRP. (a) Synthesis of organosilica NPs using a tetherable ATRP initiator as silica source in an organic solvent; (b) preparation of silica-*g*-PAN hybrids with different DPs of PAN by SI-ATRP; (c) fabrication of NPCs by carbonization of SiO_2-*g*-PAN composites and silica etching.

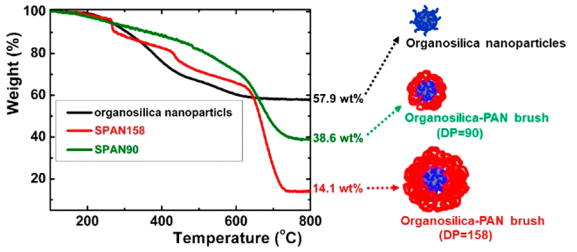

Figure 2. TGA of organosilica NPs and SiO_2-*g*-PAN with different DPs of PAN (SiPAN-158 and SiPAN-90) under air atmosphere.

complete removal of the organic component during pyrolysis. The SiO_2-*g*-PAN hybrids exhibited significant weight loss in the range from 330 to 800 °C. The weight losses were 61.4% and 85.9% for SiPAN-90 and SiPAN-158, respectively, confirming the successful PAN grafting of different lengths.

To investigate the role of PAN chain length on the microstructure of the resulting NPC, silica-*g*-PAN hybrids with different DPs of PAN were prepared by SI-ATRP. PAN chain lengths were chosen to balance high SSA (i.e., high inorganic content) with the mechanical robustness of brush particle films.[38] The degree of polymerization of grafted PAN chains was determined to be DP = 158 and 90 after HF etching of particle cores (**caution:** HF is highly corrosive, please consult materials safety data sheet prior to handling HF). In the following these samples will be referred to as SiPAN-158 and SiPAN-90, respectively. The dried SiO_2-*g*-PAN hybrids were preoxidized at 280 °C in an air flow to form a stabilized cross-linked PAN and then carbonized at 800 °C under N_2 flow.[39] NPCs derived from SiPAN-158 and SiPAN-90 were obtained after the removal of silica cores, and termed as NPC-158 and NPC-90, respectively. Figure 3 shows the representative TEM images of NPC-90 and NPC-158, revealing the highly porous structure of obtained NPCs. The pore size of the resulting NPCs was determined to be ~2.5 nm by TEM, in excellent agreement with the value deduced from N_2 sorption experiments.

The N_2 sorption isotherms of NPC-158 and NPC-90 are shown in Figure 4, which reveals a typical I behavior according to the classification of the International Union of Pure and Applied Chemistry (IUPAC) (Figure 4a).[40] Especially in lower relative pressures between 0.08 and 0.40 P/P_0, a gradual uptake

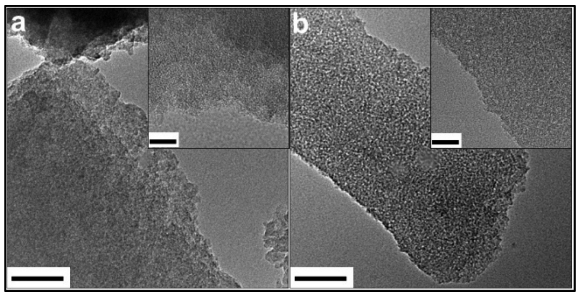

Figure 3. Representative TEM images of NPCs: (a) NPC-158 and (b) NPC-90 prepared from organosilica grafted PAN composite materials with different DPs. Insets show the enlarged images of the corresponding samples. Scale bars are 100 nm in main figures and 20 nm in insets.

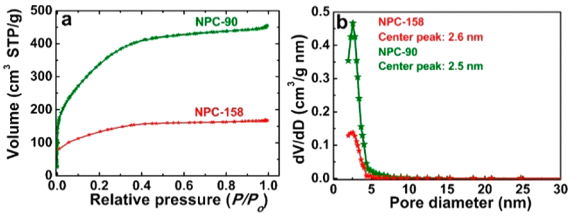

Figure 4. (a) N_2 adsorption and desorption isotherms and (b) pore size distributions of NPC-158 and NPC-90 prepared from silica-*g*-PAN with different DPs.

of N_2 is observed after the initial steepest uptake (<0.08 P/P_0), indicative of two adsorption steps, namely primary micropore filling and secondary micropore filling/capillary condensation.[41,42] The shapes of isotherms suggest the existence of massive small pores. This is further confirmed by the pore size distribution as shown in Figure 4b. Both NPCs have very narrow pore size distributions (PSD) with peak distribution at around 2.5 nm, which lies exactly on the borderline between the micropore and mesopore range. Such porosity information matches well with the TEM results. The reduction of pore size as compared to silica particle size is presumably caused by the material shrinkage during the carbonization process. A pertinent feature is the narrow size distribution of small mesopores illustrated in Figure 4b, a prerequisite for high SSA. The structural uniformity is a consequence of the "one-component" nature of particle brush hybrid materials that prevent particle aggregation and the associated more dispersed PSD. In order to clearly show the templated organosilica NPs induced mesoporosity of NPC-158 and NPC-90, pure PAN homopolymer (DP = 50) was used to prepare porous carbon for comparison. It is obvious that small mesopores between 2 and 3 nm provided the main contributions to the pore areas for both samples, indicating the uniform mesopores were templated from organosilica NPs (Figure S7).

Previously, the highest SSA measured for NPCs was 465 m^2/g when prepared using 15 nm silica NPs as the template.[34] The SSAs of NPC-158 and NPC-90 were 467 and 1244 m^2/g (calculated in 0.05−0.30 P/P_0, which is a universal range for comparison between different samples), respectively. More accurate SSAs excluding the secondary micropore filling/capillary condensation factor were calculated in lower relative pressure range (0−0.06 P/P_0), and determined to be 442 and 1020 m^2/g correspondingly. The increased SSA of NPC-90 as compared to NPC-158 is consistent with the respective increase of PAN-volume fraction and demonstrates the

DOI: 10.1021/acs.chemmater.8b00577
Chem. Mater. 2018, 30, 2208−2212

feasibility to design SSA by choosing appropriate compositions of brush particles. The SSA of NPC-90 is the highest SSA reported to date for porous carbons prepared using PAN grafted particles as the carbon precursor.[35,43−46]

The nitrogen content of NPC-90 was determined by elemental analysis to be 11.9 wt %, which was comparable with the result of X-ray photoelectron spectroscopic (XPS) analysis, indicating the uniformity of nitrogen distribution throughout the entire porous carbon.[47] The calculated surface molar ratio of pyridinic-N (N−P), pyrrolic-/pyridonic-N (N−X), and pyridine oxide (N−O) was N−P (31.1%), N−X (55.2%), and N−O (13.7%), respectively (Figures S8 and S9). The planar structured N−P located at the edge of the graphitic carbon layer provide the main initial active sites for electrochemical behaviors.[48,49] Therefore, the electrochemical performance of supercapacitors based on NPC-90 was directly evaluated by the galvanostatic charge−discharge method. The cyclic voltammetry (CV), galvanostatic charge/discharge (GCD), and electrochemical impedance spectroscopy (EIS) measurements were conducted on a model CHI660D electrochemical workstation (CH instruments).

Figure 5a shows the representative CV curves at scan rates in the range of 5 and 100 mV/s. All the curves exhibit a

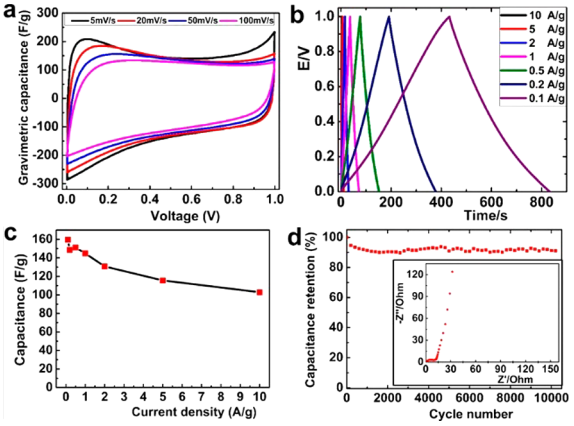

Figure 5. Electrochemical capacitive behavior of NPC-90 measured in a two-electrode system by using 6 mol/L KOH aqueous solution as electrolyte within the potential range of 0.1 to 1.0 V. (a) Cyclic voltammetry (CV) curves at various scan rates, (b) galvanostatic charge−discharge curves at different current densities, (c) specific capacitance as a function of current density ranging from 0.1 to 10 A/g, and (d) cycle durability at a current load of 2 A/g; inset shows the Nyquist plot.

rectangular shape without the presence of redox peaks, demonstrating ideal electrical double-layer capacitors (EDLCs) with a fast charging−discharging process.[50] The CV curve at the highest scan rate of 100 mV/s almost retains the initial rectangular shape measured at 5 mV/s, indicating good electrochemical performance. Figure 5b shows the GCD curves of the device at various current densities ranging from 0.1 to 10 A/g. All charge−discharge curves are linear and symmetrical with a gradual slope change at various current densities. This is a typical characteristic expected from ideal EDLCs, which is also consistent with the CV results. Plots of voltage versus time for the supercapacitors at different current densities of 0.1−10 A/g are displayed in Figure 5c. As expected, the discharge curves of the carbon capacitors are symmetrical with the corresponding charge curves. The typical triangular profiles confirm good electrochemical capacitive properties with a specific capacitance of ∼160 F/g at a current density of 100 mA/g.

EIS was employed to further study the electrochemical characteristics of NPC-based supercapacitors. The cycle durability during charge−discharge cycles of two-electrode cells made from NPC-90 electrodes was tested between 0 and 1 V at 2 A/g over 10 000 cycles. Figure 5d shows the recycling stability of NPC-90 by galvanostatic charge/discharge at a current density of 2 A/g for 10 000 cycles. A slight decrease of capacitance at initial 1000 cycles was probably related to wettability and stability of the electrodes. The capacitance increased slightly after 3000 cycles and became stable with about 91% retention, thereby exhibiting excellent stability during galvanostatic charge−discharge cycling after 10 000 cycles. As demonstrated in the inset of Figure 5d, the Nyquist plot indicates a notably rapid charge transfer process at the electrode−electrolyte interface. Moreover, the slope of the straight segment is nearly vertical to the real axis in the low-frequency region, implying nearly ideal capacitive characteristics of the NPC-based EDLCs.[51]

In addition, synthesized carbons were tested in oxygen reduction reaction (ORR) electrocatalysis. NPC-90 was deposited on a glassy carbon electrode and used as working electrode in a typical three-electrode setup with 0.1 M KOH electrolyte. As shown in Figure S10, a CV curve recorded under inert conditions did not exhibit any redox behavior. Under oxygen flow, the emergence of a strong reduction wave with onset potential −0.15 V vs Ag/AgCl was clearly observed, suggesting high ORR activity of the NPC, as usually encountered in N-doped carbon materials.[4]

To conclude, a two-step procedure for the hard-template-assisted synthesis of NPC with SSA > 1200 m^2/g and high nitrogen content (11.9 wt %) was developed. The process is based on the synthesis of bromide-containing nanosized organosilica and subsequent PAN grafting by SI-ATRP. The process alleviates the need of initiator coupling and purification and allows control of the SSA by adjustment of the molecular composition of brush particle precursors. When evaluated as an electrode material for supercapacitors, the N-enriched NPCs exhibited high capacity, good rate capability, and excellent stability during GCD cycling. We envision that the optimization of the porosity and functionality of NPCs should further enhance their performance in a number of applications, including supercapacitor electrodes, oxygen reduction reaction, catalyst supports for fuel cells, and CO_2 capture.

■ ASSOCIATED CONTENT

Supporting Information

The Supporting Information is available free of charge on the ACS Publications website at DOI: 10.1021/acs.chemmater.8b00577.

Experimental details and characterization results from TGA, TEM, DLS, CV curve, and XPS spectrum (PDF)

■ AUTHOR INFORMATION

Corresponding Authors

*K. Matyjaszewski. E-mail: km3b@anrew.cmu.edu.
*M. R. Bockstaller. E-mail: bockstaller@cmu.edu.

ORCID

Jianan Zhang: 0000-0003-3195-9882
Jiajun Yan: 0000-0003-3286-3268

DOI: 10.1021/acs.chemmater.8b00577
Chem. Mater. 2018, 30, 2208−2212

Tomasz Kowalewski: 0000-0002-3544-554X
Krzysztof Matyjaszewski: 0000-0003-1960-3402
Michael R. Bockstaller: 0000-0001-9046-9539

Notes

The authors declare no competing financial interest.

■ ACKNOWLEDGMENTS

M.R.B. and K.M. acknowledge financial support by the National Science Foundation (via grant CMMI-1662305, DMR-1410845, DMR-1501324 and DMR-1411046), National Science Center (UMO-2014/14/A/ST5/00204), as well as the Department of Energy (via DE-EE0006702). J.Z. acknowledges scholarship support by the China Scholarship Council (CSC) as well as by the Scott Institute for Energy Innovation at Carnegie Mellon University. The authors further acknowledge use of the Materials Characterization Facility at Carnegie Mellon University supported by grant MCF-677785. The authors thank Prof. Michal Kruk for his very valuable suggestions.

■ REFERENCES

(1) Yu, J.-S.; Kang, S.; Yoon, S. B.; Chai, G. Fabrication of Ordered Uniform Porous Carbon Networks and Their Application to a Catalyst Supporter. *J. Am. Chem. Soc.* **2002**, *124* (32), 9382−9383.
(2) Hasegawa, G.; Kanamori, K.; Kiyomura, T.; Kurata, H.; Abe, T.; Nakanishi, K. Hierarchically Porous Carbon Monoliths Comprising Ordered Mesoporous Nanorod Assemblies for High-Voltage Aqueous Supercapacitors. *Chem. Mater.* **2016**, *28* (11), 3944−3950.
(3) Roberts, A. D.; Li, X.; Zhang, H. Porous Carbon Spheres and Monoliths: Morphology Control, Pore Size Tuning and Their Applications as Li-Ion Battery Anode Materials. *Chem. Soc. Rev.* **2014**, *43* (13), 4341−4356.
(4) Dai, L.; Xue, Y.; Qu, L.; Choi, H. J.; Baek, J. B. Metal-Free Catalysts for Oxygen Reduction Reaction. *Chem. Rev.* **2015**, *115* (11), 4823−92.
(5) Lin, T.; Chen, I.-W.; Liu, F.; Yang, C.; Bi, H.; Xu, F.; Huang, F. Nitrogen-Doped Mesoporous Carbon of Extraordinary Capacitance for Electrochemical Energy Storage. *Science* **2015**, *350* (6267), 1508−1513.
(6) Wang, G. H.; Deng, X.; Gu, D.; Chen, K.; Tüysüz, H.; Spliethoff, B.; Bongard, H. J.; Weidenthaler, C.; Schmidt, W.; Schüth, F. Co_3O_4 Nanoparticles Supported on Mesoporous Carbon for Selective Transfer Hydrogenation of A,B-Unsaturated Aldehydes. *Angew. Chem.* **2016**, *128* (37), 11267−11271.
(7) Li, W.; Liu, J.; Zhao, D. Mesoporous Materials for Energy Conversion and Storage Devices. *Nature Reviews Materials* **2016**, *1* (6), 16023.
(8) Song, Y.; Ye, G.; Wang, Z.; Kopeć, M.; Xie, G.; Yuan, R.; Chen, J.; Kowalewski, T.; Wang, J.; Matyjaszewski, K. Controlled Preparation of Well-Defined Mesoporous Carbon/Polymer Hybrids via Surface-Initiated ICAR ATRP with a High Dilution Strategy Assisted by Facile Polydopamine Chemistry. *Macromolecules* **2016**, *49* (23), 8943−8950.
(9) McGann, J. P.; Zhong, M.; Kim, E. K.; Natesakhawat, S.; Jaroniec, M.; Whitacre, J. F.; Matyjaszewski, K.; Kowalewski, T. Block Copolymer Templating as a Path to Porous Nanostructured Carbons with Highly Accessible Nitrogens for Enhanced (Electro)Chemical Performance. *Macromol. Chem. Phys.* **2012**, *213* (10−11), 1078−1090.
(10) Zhong, M.; Kim, E. K.; McGann, J. P.; Chun, S.-E.; Whitacre, J. F.; Jaroniec, M.; Matyjaszewski, K.; Kowalewski, T. Electrochemically Active Nitrogen-Enriched Nanocarbons with Well-Defined Morphology Synthesized by Pyrolysis of Self-Assembled Block Copolymer. *J. Am. Chem. Soc.* **2012**, *134* (36), 14846−14857.
(11) Tang, C.; Tracz, A.; Kruk, M.; Zhang, R.; Smilgies, D.-M.; Matyjaszewski, K.; Kowalewski, T. Long-Range Ordered Thin Films of Block Copolymers Prepared by Zone-Casting and Their Thermal Conversion into Ordered Nanostructured Carbon. *J. Am. Chem. Soc.* **2005**, *127* (19), 6918−6919.
(12) Yuan, R.; Kopeć, M.; Xie, G.; Gottlieb, E.; Mohin, J. W.; Wang, Z.; Lamson, M.; Kowalewski, T.; Matyjaszewski, K. Mesoporous Nitrogen-Doped Carbons from Pan-Based Molecular Bottlebrushes. *Polymer* **2017**, *126*, 352−359.
(13) Liu, J.; Yang, T.; Wang, D.-W.; Lu, G. Q. M.; Zhao, D.; Qiao, S. Z. A Facile Soft-Template Synthesis of Mesoporous Polymeric and Carbonaceous Nanospheres. *Nat. Commun.* **2013**, *4*, 2798.
(14) Kopeć, M.; Yuan, R.; Gottlieb, E.; Abreu, C. M.; Song, Y.; Wang, Z.; Coelho, J. F.; Matyjaszewski, K.; Kowalewski, T. Polyacrylonitrile-B-Poly (Butyl Acrylate) Block Copolymers as Precursors to Mesoporous Nitrogen-Doped Carbons: Synthesis and Nanostructure. *Macromolecules* **2017**, *50* (7), 2759−2767.
(15) Pyun, J.; Matyjaszewski, K.; Kowalewski, T.; Savin, D.; Patterson, G.; Kickelbick, G.; Huesing, N. Synthesis of Well-Defined Block Copolymers Tethered to Polysilsesquioxane Nanoparticles and Their Nanoscale Morphology on Surfaces. *J. Am. Chem. Soc.* **2001**, *123* (38), 9445−9446.
(16) Han, B.-H.; Zhou, W.; Sayari, A. Direct Preparation of Nanoporous Carbon by Nanocasting. *J. Am. Chem. Soc.* **2003**, *125* (12), 3444−3445.
(17) Zhang, J.; Song, Y.; Kopeć, M.; Lee, J.; Wang, Z.; Liu, S.; Yan, J.; Yuan, R.; Kowalewski, T.; Bockstaller, M. R.; Matyjaszewski, K. Facile Aqueous Route to Nitrogen-Doped Mesoporous Carbons. *J. Am. Chem. Soc.* **2017**, *139* (37), 12931−12934.
(18) Zhang, J.; Yuan, R.; Natesakhawat, S.; Wang, Z.; Zhao, Y.; Yan, J.; Liu, S.; Lee, J.; Luo, D.; Gottlieb, E.; Kowalewski, T.; Bockstaller, M. R.; Matyjaszewski, K. Individual Nanoporous Carbon Spheres with High Nitrogen Content from Polyacrylonitrile Nanoparticles with Sacrificial Protective Layers. *ACS Appl. Mater. Interfaces* **2017**, *9* (43), 37804−37812.
(19) Liang, H. W.; Zhuang, X.; Brüller, S.; Feng, X.; Müllen, K. Hierarchically Porous Carbons with Optimized Nitrogen Doping as Highly Active Electrocatalysts for Oxygen Reduction. *Nat. Commun.* **2014**, *5* (5), 4973.
(20) Wang, G.; Sun, Y.; Li, D.; Liang, H. W.; Dong, R.; Feng, X.; Müllen, K. Controlled Synthesis of N-Doped Carbon Nanospheres with Tailored Mesopores through Self-Assembly of Colloidal Silica. *Angew. Chem., Int. Ed.* **2015**, *54* (50), 15191−15196.
(21) Li, Z.; Wu, D.; Liang, Y.; Fu, R.; Matyjaszewski, K. Synthesis of Well-Defined Microporous Carbons by Molecular-Scale Templating with Polyhedral Oligomeric Silsesquioxane Moieties. *J. Am. Chem. Soc.* **2014**, *136* (13), 4805−4808.
(22) Lu, A.; Kiefer, A.; Schmidt, W.; Schüth, F. Synthesis of Polyacrylonitrile-Based Ordered Mesoporous Carbon with Tunable Pore Structures. *Chem. Mater.* **2004**, *16* (1), 100−103.
(23) Jun, S.; Joo, S. H.; Ryoo, R.; Kruk, M.; Jaroniec, M.; Liu, Z.; Ohsuna, T.; Terasaki, O. Synthesis of New, Nanoporous Carbon with Hexagonally Ordered Mesostructure. *J. Am. Chem. Soc.* **2000**, *122* (43), 10712−10713.
(24) Tang, J.; Salunkhe, R. R.; Liu, J.; Torad, N. L.; Imura, M.; Furukawa, S.; Yamauchi, Y. Thermal Conversion of Core−Shell Metal−Organic Frameworks: A New Method for Selectively Functionalized Nanoporous Hybrid Carbon. *J. Am. Chem. Soc.* **2015**, *137* (4), 1572−1580.
(25) von Werne, T.; Patten, T. E. Atom Transfer Radical Polymerization from Nanoparticles: A Tool for the Preparation of Well-Defined Hybrid Nanostructures and for Understanding the Chemistry of Controlled/"Living" Radical Polymerizations from Surfaces. *J. Am. Chem. Soc.* **2001**, *123* (31), 7497−7505.
(26) Pyun, J.; Matyjaszewski, K. Synthesis of Nanocomposite Organic/Inorganic Hybrid Materials Using Controlled/"Living" Radical Polymerization. *Chem. Mater.* **2001**, *13* (10), 3436−3448.
(27) Matyjaszewski, K.; Tsarevsky, N. V. Nanostructured Functional Materials Prepared by Atom Transfer Radical Polymerization. *Nat. Chem.* **2009**, *1* (4), 276−288.
(28) Matyjaszewski, K.; Xia, J. Atom Transfer Radical Polymerization. *Chem. Rev.* **2001**, *101* (9), 2921−2990.

DOI: 10.1021/acs.chemmater.8b00577
Chem. Mater. 2018, 30, 2208−2212

(29) Chen, W.-L.; Cordero, R.; Tran, H.; Ober, C. K. 50th Anniversary Perspective: Polymer Brushes: Novel Surfaces for Future Materials. *Macromolecules* **2017**, *50* (11), 4089−4113.
(30) Edmondson, S.; Osborne, V. L.; Huck, W. T. Polymer Brushes via Surface-Initiated Polymerizations. *Chem. Soc. Rev.* **2004**, *33* (1), 14−22.
(31) Matyjaszewski, K. Atom Transfer Radical Polymerization (ATRP): Current Status and Future Perspectives. *Macromolecules* **2012**, *45* (10), 4015−4039.
(32) Hui, C. M.; Pietrasik, J.; Schmitt, M.; Mahoney, C.; Choi, J.; Bockstaller, M. R.; Matyjaszewski, K. Surface-Initiated Polymerization as an Enabling Tool for Multifunctional (Nano-) Engineered Hybrid Materials. *Chem. Mater.* **2014**, *26* (1), 745−762.
(33) Wu, D.; Li, Z.; Zhong, M.; Kowalewski, T.; Matyjaszewski, K. Templated Synthesis of Nitrogen-Enriched Nanoporous Carbon Materials from Porogenic Organic Precursors Prepared by ATRP. *Angew. Chem.* **2014**, *126* (15), 4038−4041.
(34) Tang, C.; Bombalski, L.; Kruk, M.; Jaroniec, M.; Matyjaszewski, K.; Kowalewski, T. Nanoporous Carbon Films from "Hairy" Polyacrylonitrile-Grafted Colloidal Silica Nanoparticles. *Adv. Mater.* **2008**, *20* (8), 1516−1522.
(35) Wu, D.; Dong, H.; Pietrasik, J.; Kim, E. K.; Hui, C. M.; Zhong, M.; Jaroniec, M.; Kowalewski, T.; Matyjaszewski, K. Novel Nanoporous Carbons from Well-Defined Poly (Styrene-Co-Acrylonitrile)-Grafted Silica Nanoparticles. *Chem. Mater.* **2011**, *23* (8), 2024−2026.
(36) Cao, L.; Kruk, M. Ordered Arrays of Hollow Carbon Nanospheres and Nanotubules from Polyacrylonitrile Grafted on Ordered Mesoporous Silicas Using Atom Transfer Radical Polymerization. *Polymer* **2015**, *72*, 356−360.
(37) Hui, C. M.; Dang, A.; Chen, B.; Yan, J.; Konkolewicz, D.; He, H.; Ferebee, R.; Bockstaller, M. R.; Matyjaszewski, K. Effect of Thermal Self-Initiation on the Synthesis, Composition, and Properties of Particle Brush Materials. *Macromolecules* **2014**, *47* (16), 5501−5508.
(38) Schmitt, M.; Choi, J.; Hui, C. M.; Chen, B.; Korkmaz, E.; Yan, J.; Margel, S.; Ozdoganlar, O. B.; Matyjaszewski, K.; Bockstaller, M. R. Processing Fragile Matter: Effect of Polymer Graft Modification on the Mechanical Properties and Processibility of (Nano-) Particulate Solids. *Soft Matter* **2016**, *12* (15), 3527−3537.
(39) Liu, X.; Chen, W.; Hong, Y.-l.; Yuan, S.; Kuroki, S.; Miyoshi, T. Stabilization of Atactic-Polyacrylonitrile under Nitrogen and Air as Studied by Solid-State Nmr. *Macromolecules* **2015**, *48* (15), 5300−5309.
(40) Sing, K. S. Reporting Physisorption Data for Gas/Solid Systems with Special Reference to the Determination of Surface Area and Porosity (Recommendations 1984). *Pure Appl. Chem.* **1985**, *57* (4), 603−619.
(41) Kakei, K.; Ozeki, S.; Suzuki, T.; Kaneko, K. Multi-Stage Micropore Filling Mechanism of Nitrogen on Microporous and Micrographitic Carbons. *J. Chem. Soc., Faraday Trans.* **1990**, *86* (2), 371−376.
(42) Ravikovitch, P. I.; Domhnaill, S. C. O.; Neimark, A. V.; Schueth, F.; Unger, K. K. Capillary Hysteresis in Nanopores: Theoretical and Experimental Studies of Nitrogen Adsorption on Mcm-41. *Langmuir* **1995**, *11* (12), 4765−4772.
(43) Kruk, M.; Dufour, B.; Celer, E. B.; Kowalewski, T.; Jaroniec, M.; Matyjaszewski, K. Synthesis of Mesoporous Carbons Using Ordered and Disordered Mesoporous Silica Templates and Polyacrylonitrile as Carbon Precursor. *J. Phys. Chem. B* **2005**, *109* (19), 9216−9225.
(44) Kruk, M.; Dufour, B.; Celer, E. B.; Kowalewski, T.; Jaroniec, M.; Matyjaszewski, K. Well-Defined Poly (Ethylene Oxide)-Polyacrylonitrile Diblock Copolymers as Templates for Mesoporous Silicas and Precursors for Mesoporous Carbons. *Chem. Mater.* **2006**, *18* (6), 1417−1424.
(45) Kim, C.; Ngoc, B. T. N.; Yang, K. S.; Kojima, M.; Kim, Y. A.; Kim, Y. J.; Endo, M.; Yang, S. C. Self-Sustained Thin Webs Consisting of Porous Carbon Nanofibers for Supercapacitors via the Electrospinning of Polyacrylonitrile Solutions Containing Zinc Chloride. *Adv. Mater.* **2007**, *19* (17), 2341−2346.
(46) Zhong, M.; Natesakhawat, S.; Baltrus, J. P.; Luebke, D.; Nulwala, H.; Matyjaszewski, K.; Kowalewski, T. Copolymer-Templated Nitrogen-Enriched Porous Nanocarbons for CO_2 Capture. *Chem. Commun.* **2012**, *48* (94), 11516−11518.
(47) Ju, M. J.; Choi, I. T.; Zhong, M.; Lim, K.; Ko, J.; Mohin, J.; Lamson, M.; Kowalewski, T.; Matyjaszewski, K.; Kim, H. K. Copolymer-Templated Nitrogen-Enriched Nanocarbons as a Low Charge-Transfer Resistance and Highly Stable Alternative to Platinum Cathodes in Dye-Sensitized Solar Cells. *J. Mater. Chem. A* **2015**, *3* (8), 4413−4419.
(48) Wickramaratne, N. P.; Xu, J.; Wang, M.; Zhu, L.; Dai, L.; Jaroniec, M. Nitrogen Enriched Porous Carbon Spheres: Attractive Materials for Supercapacitor Electrodes and CO_2 Adsorption. *Chem. Mater.* **2014**, *26* (9), 2820−2828.
(49) Tan, Z.; Ni, K.; Chen, G.; Zeng, W.; Tao, Z.; Ikram, M.; Zhang, Q.; Wang, H.; Sun, L.; Zhu, X.; Wu, X.; Ji, H.; Ruoff, R. S.; Zhu, Y. Incorporating Pyrrolic and Pyridinic Nitrogen into a Porous Carbon Made from C_{60} Molecules to Obtain Superior Energy Storage. *Adv. Mater.* **2017**, *29* (8), 1603414.
(50) Conway, B. E. *Electrochemical Supercapacitors: Scientific Fundamentals and Technological Applications*; Springer Science & Business Media, 2013.
(51) Miao, F.; Shao, C.; Li, X.; Wang, K.; Lu, N.; Liu, Y. Three-Dimensional Freestanding Hierarchically Porous Carbon Materials as Binder-Free Electrodes for Supercapacitors: High Capacitive Property and Long-Term Cycling Stability. *J. Mater. Chem. A* **2016**, *4* (15), 5623−5631.

DOI: 10.1021/acs.chemmater.8b00577
Chem. Mater. 2018, 30, 2208−2212